Angewandte Chemie
Eine Zeitschrift der Gesellschaft Deutscher Chemiker

Supporting Information

69451 Weinheim, Germany

Selective Capture of Carbon Dioxide under Humid Conditions by Hydrophobic Chabazite-Type Zeolitic Imidazolate Frameworks**

*Nhung T. T. Nguyen, Hiroyasu Furukawa, Felipe Gándara, Hoang T. Nguyen, Kyle E. Cordova, and Omar M. Yaghi**

anie_201403980_sm_miscellaneous_information.pdf

Section S1: General Methods and Synthesis of ZIF-300, -301, and -302

Methods:

Chemicals used in this work. 5(6)-bromobenzimidazole (bbImH), 5(6)-chlorobenzimidazole (cbImH), 5(6)-methylbenzimidazole (mbImH), *N*,*N*-dimethylformamide (DMF) were purchased from the Aldrich Chemical Co. and anhydrous methanol was obtained from Acros Organics. 2-methylimidazole (2-mImH) and zinc nitrate tetrahydrate were purchased from Merck Chemical Co. All of these chemicals were used without further purification. All experiments were performed in air.

Analytical techniques. Single crystal data were collected on a Bruker D8 Venture diffractometer using monochromatic fine focus Cu Kα radiation (λ = 1.54178 Å) operated at 50 kW and 1.0 mA and APEX II detector. Additional data was collected using synchrotron radiation in the beam line 11.3.1 of the Advanced Light Source, LBNL (SI, Section S2). Solution ^{1}H NMR spectra were acquired on a Bruker AVB-400 NMR spectrometer (SI, Section S3). SEM images were taken on a Hitachi S-4800 scanning electron microscope operating at an accelerating voltage of 1 kV (SI, Section S4). Powder X-ray data were collected using a Bruker D8 Advancer employing Ni filtered Cu Kα (λ = 1.54178 Å). The system was also outfitted with an anti-scattering shield that prevents incident diffuse radiation from hitting the detector. Samples were placed on zero background sample holders by dropping powders from a spatula and then leveling the sample with a spatula. The 2θ range was 3-50° with a step size of 0.02° and a fixed counting time of 1 s/step (SI, Section S5). Thermal gravimetric analysis (TGA) curves were recorded on a TA Q500 thermal analysis system under air flow (SI, Section S6). Elemental microanalyses (EA) were performed in the Microanalytical Laboratory of the College of Chemistry at UC Berkeley, using a Perkin Elmer 2400 Series II CHNS elemental analyzer. FT-IR spectra were measured from KBr pellets using a Bruker Vertex 70 system. Low-pressure Ar adsorption isotherms were recorded on a Quantachrome Autosorb-1 volumetric gas adsorption analyzer. Liquid argon baths were used for the measurements at 87 K, respectively (SI, Section S7). Water (SI, Section S8), CO_2, and N_2 isotherms (SI, section S9) were measured on a Quantachrome Autosorb-iQ2. The measurement temperature was controlled with a water circulator. Helium was used for the estimation of dead space for gas and water adsorption measurements. Ultra-high-purity grade N_2, Ar, and He gases (99.999% purity), CO_2 (99.995%) were used throughout the experiments.

Synthesis and Characterization of ZIFs:

$Zn(2\text{-}mIm)_{0.86}(bbIm)_{1.14}\cdot(DMF)_{0.09}$, ZIF-300: 2-mImH (11.7 mg, 0.143 mmol), bbImH (28.2 mg, 0.143 mmol), and $Zn(NO_3)_2\cdot 4H_2O$ (29.8 mg, 0.114 mmol) were dissolved in a solvent mixture of DMF (4.75 mL) and water (0.25 mL) in a 8-mL capped vial. The vial was heated at 120 °C for 3 days. The light brown block shaped crystals were collected and washed with DMF (5 × 3 mL) for one day (yield 47% based on the amount of zinc salt).

After the initial DMF washing, as-synthesized samples of ZIF-300 were solvent exchanged three times per day with dry methanol at ambient temperature over a total of 3 days. Finally at the end of the third day, the methanol was decanted and the resulting solvent-exchanged samples were evacuated (10 mTorr) at ambient temperature for 24 h, followed by subsequent heating at 180 °C for 2 h to yield activated sample. EA of activated sample: Calcd. for $ZnC_{11.70}H_{9.397}N_{4.093}O_{0.093}Br_{1.143}$ = Zn $(2\text{-}mIm)_{0.86}(bbIm)_{1.14}\cdot(DMF)_{0.09}$: C, 38.40; H, 2.60; N, 15.67%. Found: C, 38.41; H, 2.40; N, 15.49%. FT-IR (KBr, 4000–400 cm^{-1}): 2925 (w), 1868 (w), 1771 (w), 1673 (m), 1604 (m), 1572 (w), 1471 (s), 1460 (s), 1430 (s), 1378 (w), 1339 (m), 1308 (w), 1288 (s), 1251 (s), 1238 (s), 1190 (s), 1178 (s), 1145 (s), 1128 (m), 1090 (w), 1051 (m), 993 (m), 951 (s), 890 (w), 855 (m), 803 (s), 794 (s), 755 (s), 705 (s), 688 (s), 648 (s).

$Zn(2\text{-}mIm)_{0.94}(cbIm)_{1.06}\cdot(DMF)_{0.03}$, ZIF-301: 2-mImH (11.7 mg, 0.143 mmol), cbImH (21.8 mg, 0.143 mmol), and $Zn(NO_3)_2\cdot 4H_2O$ (29.8 mg, 0.114 mmol) were dissolved in a solvent mixture of DMF (4.75 mL) and water (0.25 mL) in a 8-mL capped vial. The vial was heated at 120 °C for 3 days. The colorless crystals were collected and washed with DMF (5 × 3 mL) for one day (yield 47% based on the total amounts of zinc salt).

After the initial DMF washing, as-synthesized samples of ZIF-301 were solvent exchanged three times per day with dry methanol at ambient temperature over a total of 3 days. Finally at the end of the third day, the methanol was decanted and the resulting solvent-exchanged samples were evacuated (10 mTorr) at ambient temperature for 24 h, followed by subsequent heating at 180 °C for 2 h to yield activated sample. EA of activated sample: Calcd. for $ZnC_{11.26}H_{9.125}N_{4.03}O_{0.03}Cl_{1.055}$ = Zn $(2\text{-}mIm)_{0.94}(cbIm)_{1.06}\cdot(DMF)_{0.03}$: C, 44.42; H, 3.04; N, 18.63. Found: C, 44.19; H, 2.85; N, 18.53%. FT-IR (KBr, 4000–400 cm^{-1}): 1868 (w), 1772 (w), 1735 (w), 1610 (w), 1575 (w), 1473 (s), 1435 (w), 1421 (w), 1377 (w), 1340 (s), 1310 (m), 1289 (s), 1254 (s), 1238 (s), 1193 (s), 1179 (s), 1146 (s), 1126 (w), 1063 (w), 929 (s), 890 (m), 854 (m), 801 (s), 750 (s), 724 (s), 688 (s), 649 (s).

$Zn(2\text{-}mIm)_{0.67}(mbIm)_{1.33}\cdot(H_2O)_{0.5}$, ZIF-302: 2-mImH (9.9 mg, 0.120 mmol), mbImH (21.4 mg, 0.140 mmol), and $Zn(NO_3)_2\cdot 4H_2O$ (36.6 mg, 0.140 mmol) were dissolved in a solvent mixture of DMF (3.5 mL) and water (0.5 mL) in a 8-mL capped vial. The vial was heated at 120 °C for 3 days. The colorless crystals were collected and washed with DMF (5 × 3 mL) for a day (yield 46% based on the total amounts of links).

After the initial DMF washing, as-synthesized samples of ZIF-302 were solvent exchanged three times per day with dry methanol at ambient temperature over a total of 3 days. Finally at the end of the third day, the methanol was decanted and the resulting solvent-exchanged samples were evacuated (10 mTorr) at ambient temperature for 24 h, followed by subsequent heating at 180 °C for 2 h to yield activated sample. EA of activated sample: Calcd. for $ZnC_{13.33}H_{13.67}N_{4.0}O_{0.5}$ = $Zn(2\text{-}mIm)_{0.67}(mbIm)_{1.33}\cdot(H_2O)_{0.5}$: C, 52.79; H, 4.43; N, 18.47%. Found: C, 53; H, 4.0; N, 18.53%. FT-IR (KBr, 4000–400 cm^{-1}): 1869 (w), 1774 (w), 1716 (w), 1683 (w), 1653 (w), 1619 (w), 1605 (w), 1582 (w), 1558 (w), 1541 (w), 1472 (s), 1377 (w), 1346 (m), 1291 (s), 1242 (s), 1203 (s), 1173 (w), 1142 (s), 1131 (s), 1020.47 (w), 994 (m), 945 (m), 884 (w), 861 (w), 823 (s), 801 (s), 761 (s), 689 (s), 650 (s), 625 (s).

Section S2: Single Crystal X-ray Diffraction Analyses

ZIF-300 (CHA-TRIGONAL)

Single crystal X-ray diffraction data collection and structural solution for ZIF-300

The single crystal data for a light brown block shaped crystal (0.122 × 0.132 × 0.180 mm^3) were collected on a Bruker D8 Venture diffractometer using monochromatic fine focus Cu Kα radiation (λ = 1.54178 Å) operated at 50 kW and 1.0 mA. The crystal was cooled down to -173 °C by chilled nitrogen flow controlled by Kryoflex system. The frames were collected with an exposure of 60 sec/frame by scanning omega and phi X-ray crystallographic analysis. The frames were integrated with the Bruker SAINT software package using a narrow-frame algorithm. The integration of the data using a trigonal unit cell yielded a total of 21827 reflections to a maximum θ angle of 47.85° (1.04 Å resolution), of which 3107 were independent (average redundancy 7.025, completeness = 99.3%, R_{int} = 6.04%) and 2240 (72.10%) were greater than 2σ(F^2). The final cell constants of a = 27.631(4) Å, b = 27.631(4) Å, c = 22.827(5) Å, V = 15093.(3) $Å^3$, are based upon the refinement of the XYZ-centroids of reflections above 20 σ(I). The final anisotropic full-matrix least-squares refinement on F^2 with 287 variables converged at R_1 = 17.21%, for the observed data and wR_2 = 47.60% for all data. The goodness-of-fit was 2.156. The largest peak in the final difference electron density synthesis was 1.42 $e^- Å^{-3}$ and the largest hole was -1.047 $e^- Å^{-3}$ with an RMS deviation of 0.196 $e^- Å^{-3}$. On the basis of the final model, the calculated density was 1.351 g cm^{-3} and F(000), 5952 e^-. The low quality of the diffraction data and the low resolution, together with the different disorder in the crystal, resulted in relatively large residual values, which produced several A-alerts in the checkcif file.

Table S1. Crystal data and structure refinement for ZIF-300.

Empirical formula	$C_{396}H_{180}N_{144}Zn_{36}Br_{36}O_6$	
Formula weight	12280.85	
Temperature	100 K	
Wavelength	1.54178 Å	
Crystal system	Trigonal	
Space group	*R*-3	
Unit cell dimensions	a = 27.631(4) Å	α = 90°
	b = 27.631(4) Å	β = 90°
	c = 22.827(5) Å	ɣ = 120°
Volume	15093.(5) $Å^3$	
Z	1	
Density (calculated)	1.351 g cm^3	
Absorption coefficient	4.637 mm^{-1}	
F(000)	5952.0	
Crystal size	0.122 × 0.132 × 0.180 mm^3	
Theta range for data collection	2.675 to 47.855°	
Index ranges	$-26 \le h \le 26$, $-26 \le k \le 26$, $-21 \le l \le 21$	
Reflections collected	21827	
Independent reflections	3107 [R_{int} = 0.0604]	
Coverage of independent reflections	100%	
Absorption correction	Multi-scan	
Refinement method	Full matrix least square on F^2	
Data / restraints / parameters	3107 / 10 / 287	
Goodness-of-fit on F^2	2.156	
Final R indices [$I > 2\sigma(I)$]	R_1 = 0.1721, wR_2 = 0.4760	
R indices (all data)	R_1 = 0.2050, wR_2 = 0.4953	
Largest diff. peak and hole	1.42 and -1.05 e^- $Å^{-3}$	

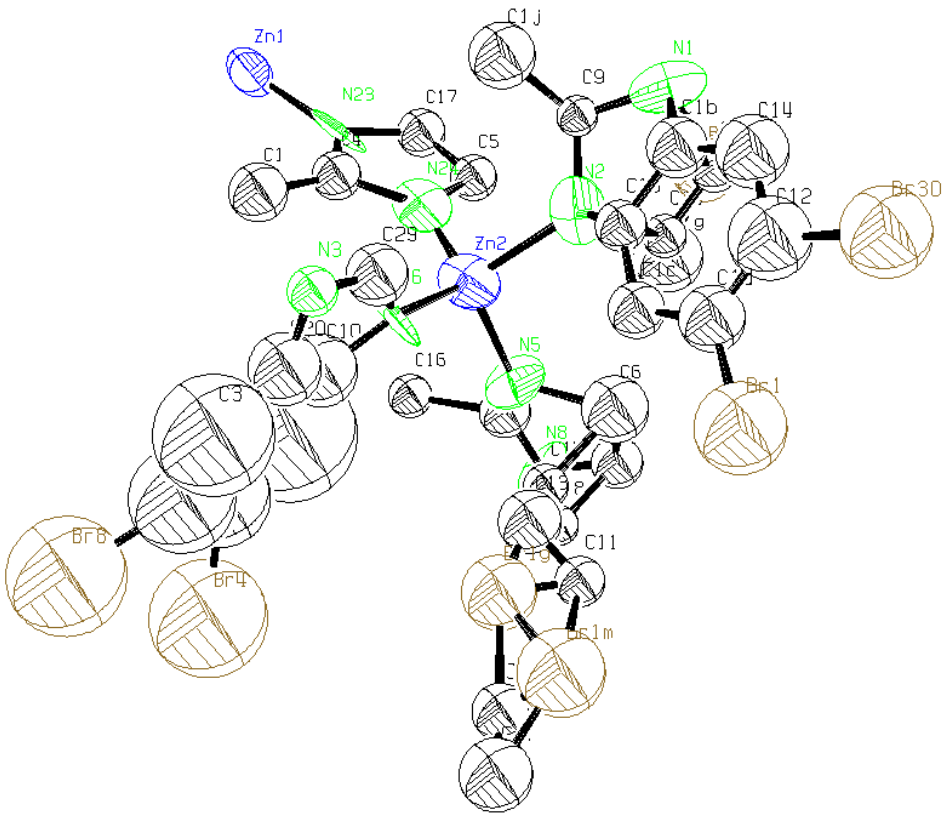

Figure S1. The asymmetric unit of ZIF-300 showing zinc surrounded by four imidazolate links with imposed disorder. The unit was drawn by ORTEP with thermal ellipsoids style at 50% probability. Hydrogen atoms were omitted for clarity.

ZIF-301 (CHA-TRIGONAL)

Single crystal X-ray diffraction data collection and structural solution for ZIF-301

The single crystal data for a colorless block shaped crystal (0.04 × 0.06 × 0.10 mm^3) were collected at the beam line 11.3.1 of the Advanced Light Source (ALS), using synchrotron radiation with wavelength λ = 0.7749 Å. The crystal was cooled down to -173 °C by chilled nitrogen flow controlled by Kryoflex system. The frames covering 0.3° were collected with an exposure of 1 sec/frame by scanning omega.

The frames were integrated with the Bruker SAINT software package using a narrow-frame algorithm. The integration of the data using a trigonal unit cell yielded a total of 28582 reflections to a maximum θ angle of 27.11° (0.85 Å resolution), of which 5321 were independent (average redundancy 5.372, completeness = 97.1%, R_{int} = 8.31%) and 3512 (66.00%) were greater than 2σ(F^2). The final cell constants of a = 27.590(6) Å, b = 27.590(6) Å, c = 21.891(4) Å, V = 14431.(6) $Å^3$, are based upon the refinement of the XYZ-centroids of reflections above 20 σ(I). The calculated minimum and maximum transmission coefficients (based on crystal size) are 0.7763 and 1.0000. The final anisotropic full-matrix least-squares refinement on F^2 with 409 variables converged at R_1 = 8.83%, for the observed data and wR_2 = 27.10% for all data. The goodness-of-fit was 1.071. The largest peak in the final difference electron density synthesis was 0.89 $e^- Å^{-3}$ and the largest hole was -0.610 $e^- Å^{-3}$ with an RMS deviation of 0.11 $e^- Å^{-3}$. On the basis of the final model, the calculated density was 1.212 g cm^{-3} and F(000), 5252 e^-. As discussed in the text, two imidazolate links are disordered. Specifically, there are two cases of occupational disorder where a molecule of 2-mIm and another of cbIm were found to occupy the same position. Their occupancies were fixed to one half for each one of them. In addition, another cbIm presented a probable dynamic disorder. It has been modeled with the phenyl rings occupying four possible positions, with 25% occupancy for each one of them. Several constraints and restraints were employed during the refinement, with the C and Cl atoms of the phenyl rings being fixed to be flat and refined with EADP.

Table S2. Crystal data and structure refinement for ZIF-301.

Empirical formula	$C_{396}H_{216}Cl_{31.5}N_{144}O_{4.5}Zn_{36}$	
Formula weight	10533.11	
Temperature	100 K	
Wavelength	0.7749 Å	
Crystal system	Trigonal	
Space group	*R*-3	
Unit cell dimensions	a = 27.590(6) Å	α = 90°
	b = 27.590(6) Å	β = 90°
	c = 21.891(4) Å	ɣ = 120°
Volume	14431.(6) $Å^3$	
Z	1	
Density (calculated)	1.2126 g cm^3	
Absorption coefficient	2.096 mm^{-1}	
F(000)	5252.0	
Crystal size	0.04 × 0.06 × 0.10 mm	
Theta range for data collection	2.66 to 27.106°	
Index ranges	$-32 \le h \le 32$, $-32 \le k \le 32$, $-25 \le l \le 25$	
Reflections collected	28582	
Independent reflections	5321 [R_{int} = 0.0831]	
Coverage of independent reflections	94.6%	
Absorption correction	Multi-scan	
Refinement method	Full matrix least square on F^2	
Data / restraints / parameters	5321 / 7 / 409	
Goodness-of-fit on F^2	1.071	
Final R indices [$I > 2\sigma(I)$]	R_1 = 0.0883, wR_2 = 0.2710	
R indices (all data)	R_1 = 0.1175, wR_2 = 0.2832	
Largest diff. peak and hole	0.89 and -0.62 e^- $Å^{-3}$	

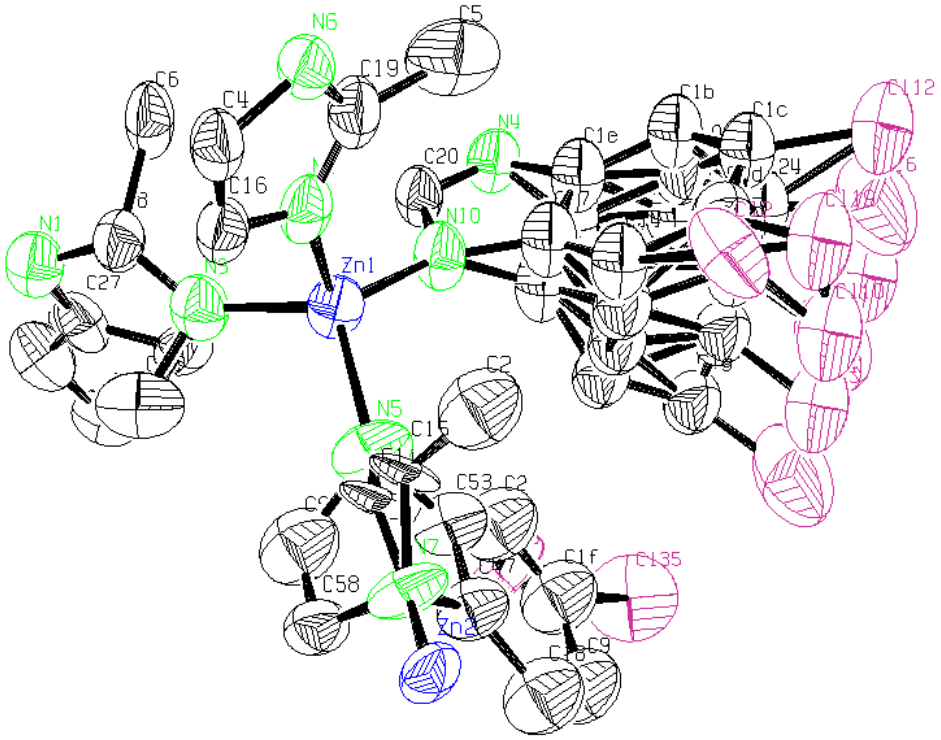

Figure S2. The asymmetric unit of ZIF-301 showing zinc surrounded by four imidazolate links with imposed disorder. The unit was drawn by ORTEP with thermal ellipsoids style at 50% probability. Hydrogen atoms were omitted for clarity.

ZIF-302 (CHA-TRIGONAL)

Single crystal X-ray diffraction data collection and structural solution for ZIF-302

Single crystal data for a colorless block shaped crystal (0.11 × 0.162 × 0.176 mm^3) were collected on a Bruker D8 Venture diffractometer using monochromatic fine focus Cu Kα radiation (λ = 1.54178 Å) operated at 50 kW and 1.0 mA. The crystal was cooled down to -173 °C by chilled nitrogen flow controlled by Kryoflex system. The frames were collected with an exposure of 60 sec/frame by scanning omega and phi X-ray crystallographic analysis. The frames were integrated with the Bruker SAINT software package using a narrow-frame algorithm. The integration of the data using a trigonal unit cell yielded a total of 24185 reflections to a maximum θ angle of 44.57° (1.10 Å resolution), of which 2663 were independent (average redundancy 9.082, completeness = 99.6%, Rint = 8.79%) and 1803 (67.71%) were greater than $2\sigma(F^2)$. The final cell constants of a = 27.653(2) Å, b = 27.653(2) Å, c = 22.9284(19) Å, V = 15184.(3) $Å^3$, are based upon the refinement of the XYZ-centroids of 8143 reflections above 20 $\sigma(I)$ with 5.341° < 2θ < 87.2°. Data were corrected for absorption effects using the multi-scan method (SADABS). The ratio of minimum to maximum apparent transmission was 0.923. The final anisotropic full-matrix least-squares refinement on F^2 with 268 variables converged at R_1 = 8.28%, for the observed data and wR_2 = 22.45% for all data. The goodness-of-fit was 1.084. The largest peak in the final difference electron density synthesis was 0.63 $e^- Å^{-3}$ and the largest hole was -0.68 $e^- Å^{-3}$ with an RMS deviation of 0.125 $e^- Å^{-3}$. On the basis of the final model, the calculated density was 1.17 g cm^{-3} and $F(000)$, 5422.0 e^-.

Table S3. Crystal data and structure refinement for ZIF-302.

Empirical formula	$C_{480}H_{351}N_{150}O_{7.6}Zn_{36}$	
Formula weight	10695.49	
Temperature	100(2) K	
Wavelength	1.54178 Å	
Crystal system	Trigonal	
Space group	*R*-3	
Unit cell dimensions	a = 27.653(2) Å	α = 90°
	b = 27.653(2) Å	β = 90°
	c = 22.9284(19) Å	ɣ = 120°
Volume	15184.(3) $Å^3$	
Z	1	
Density (calculated)	1.170 g cm^3	
Absorption coefficient	1.963 mm^{-1}	
F(000)	5422.0	
Crystal size	0.11 × 0.162 × 0.176 mm^3	
Theta range for data collection	2.67 to 44.57°	
Index ranges	$-25 \leq h \leq 25$, $-25 \leq k \leq 24$, $-20 \leq l \leq 20$	
Reflections collected	24185	
Independent reflections	2663 [R_{int} = 0.0879]	
Coverage of independent reflections	99.6%	
Absorption correction	Multi-scan	
Refinement method	Full matrix least square on F^2	
Data / restraints / parameters	2663 / 1 / 268	
Goodness-of-fit on F^2	1.083	
Final R indices [$I > 2\sigma(I)$]	R_1 = 0.0828, wR_2 = 0.2245	
R indices (all data)	R_1 = 0.1302, wR_2 = 0.2555	
Largest diff. peak and hole	0.631 and -0.677 $e^- Å^{-3}$	

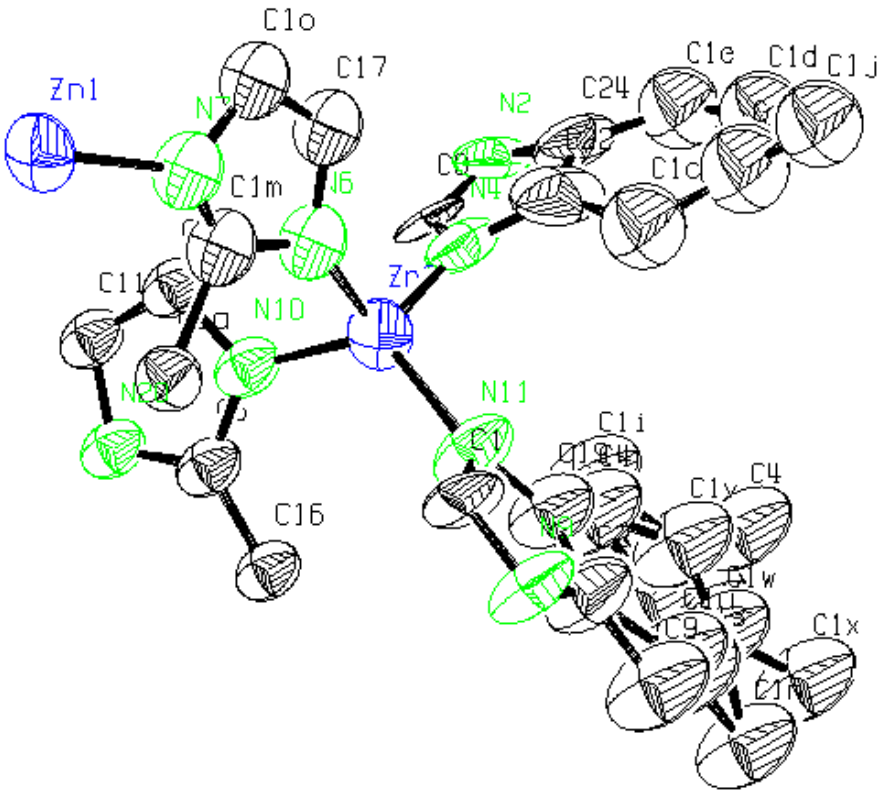

Figure S3. The asymmetric unit of ZIF-302 showing zinc surrounded by four imidazolate links with imposed disorder. The unit was drawn by ORTEP with thermal ellipsoids style at 50% probability. Hydrogen atoms were omitted for clarity.

Section S3: Proton Nuclear Magnetic Resonance Analyses

Each ZIF sample (ca. 10 mg) was placed in 30 µL of DCl (20% in D_2O) and 570 µL of DMSO-d_6 and then sonicated for ~10 min in order to fully digest the ZIF and dissolve the link constituents. The mole ratios of the links in each ZIF were calculated based on the integrations of the identifying signals.

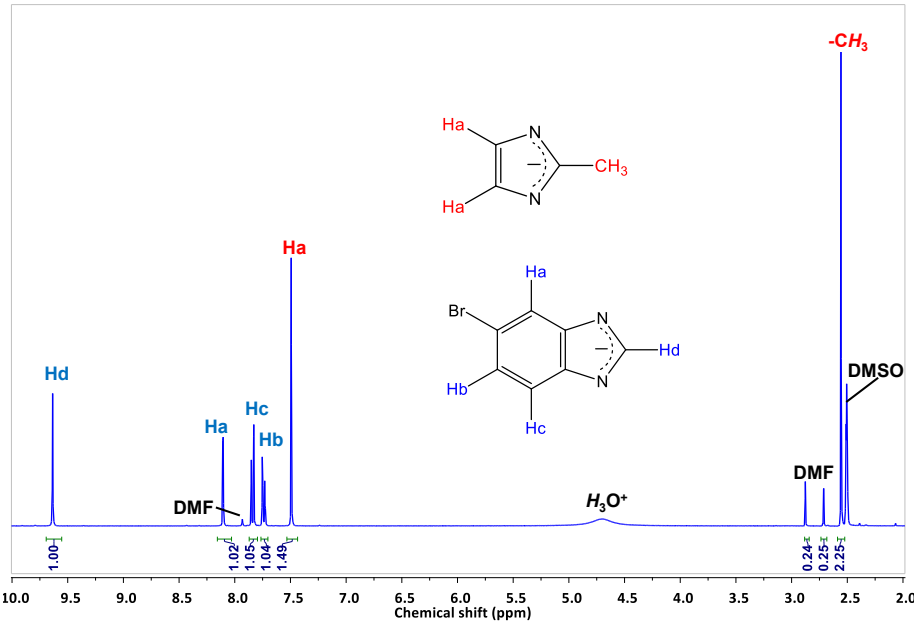

Figure S4. ^{1}H NMR spectrum of ZIF-300 post-digestion. The calculated ratio of 2-mIm : bbIm in ZIF-300 is 3 : 4.

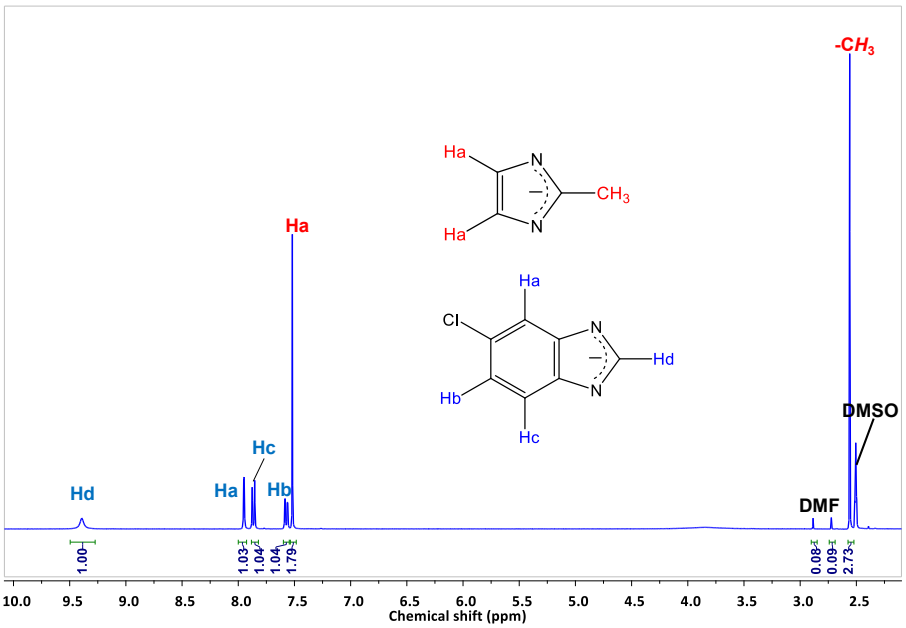

Figure S5. ^{1}H NMR spectrum of ZIF-301 post-digestion. The calculated ratio of 2-mIm : cbIm in ZIF-301 is 9 : 10.

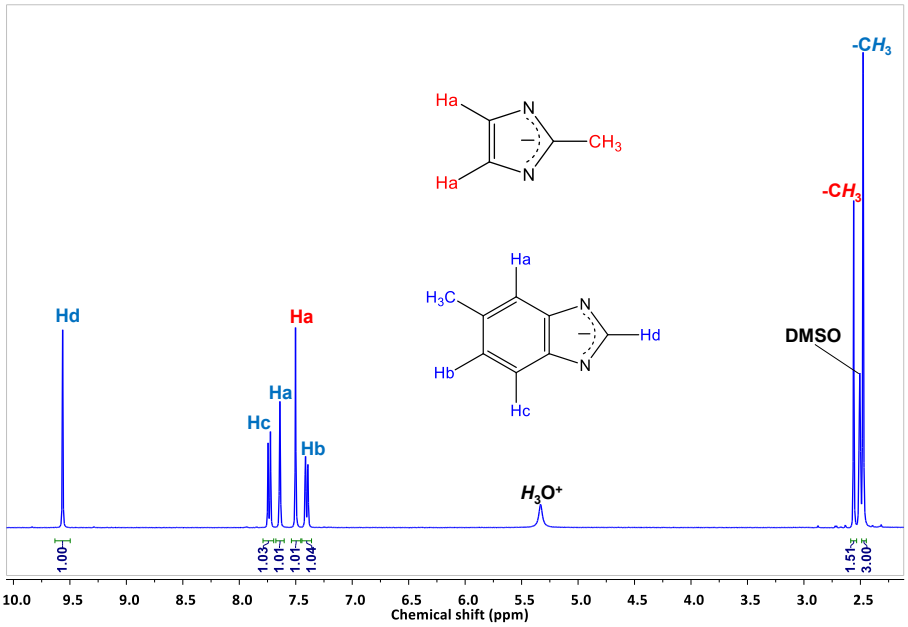

Figure S6. ^{1}H NMR spectrum of ZIF-302 post-digestion. The calculated ratio of 2-mIm : mbIm in ZIF-302 is 1 : 2.

Section S4: Scanning Electron Microscope Images

Images of as-synthesized ZIF-300, -301, and -302 were taken by dispersing each sample onto a sticky carbon surface attached to a flat aluminum sample holder.

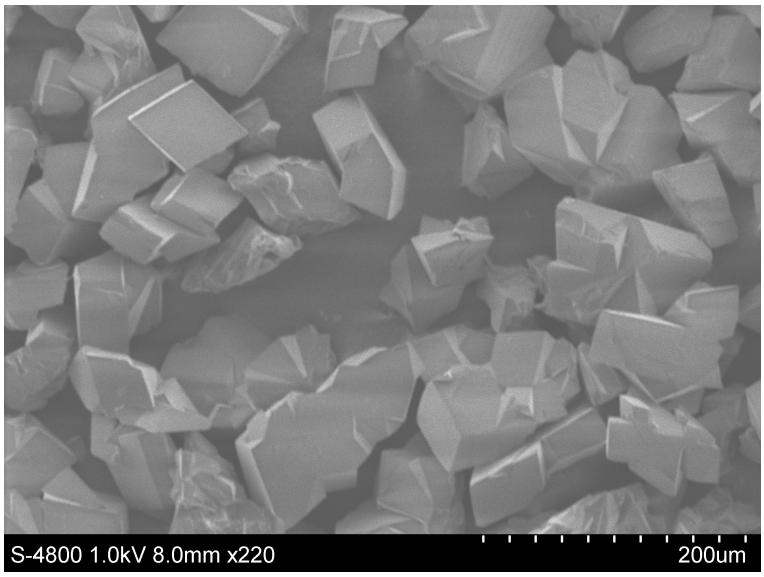

Figure S7. SEM image reveals the single-phase homogeneous morphology of as-synthesized ZIF-300.

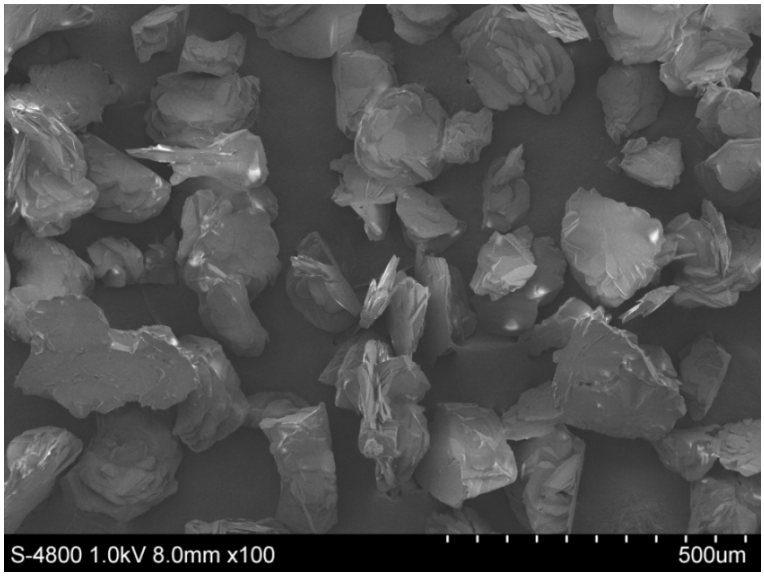

Figure S8. SEM image reveals the single-phase homogeneous morphology of as-synthesized ZIF-301.

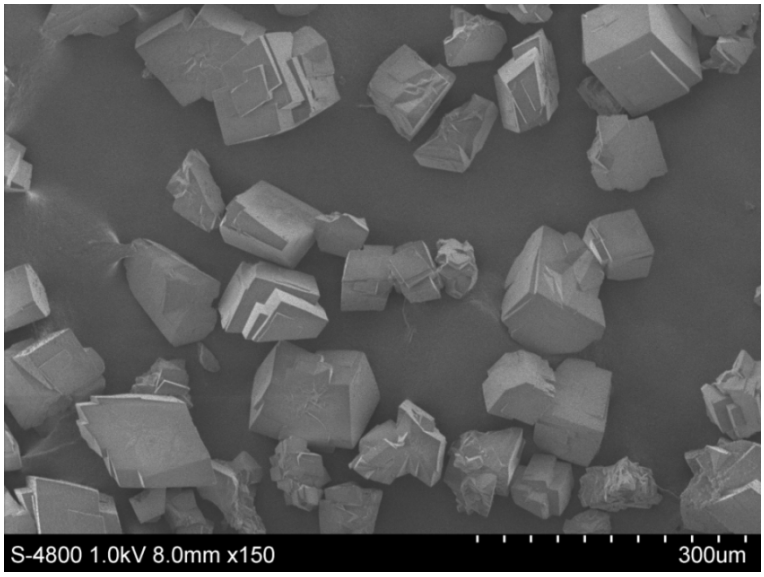

Figure S9. SEM image reveals the single-phase homogeneous morphology of as-synthesized ZIF-302.

Section S5: Powder X-ray Diffraction Patterns

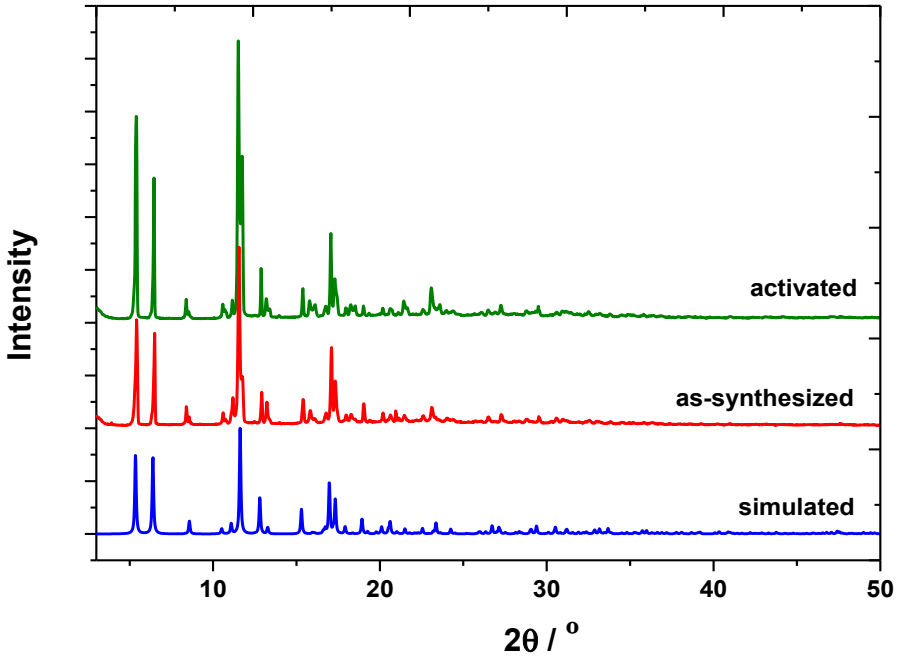

Figure S10. Comparison of the simulated (blue) PXRD pattern with the experimental as-synthesized (red) and activated [guest-free, (green)] PXRD patterns of ZIF-300.

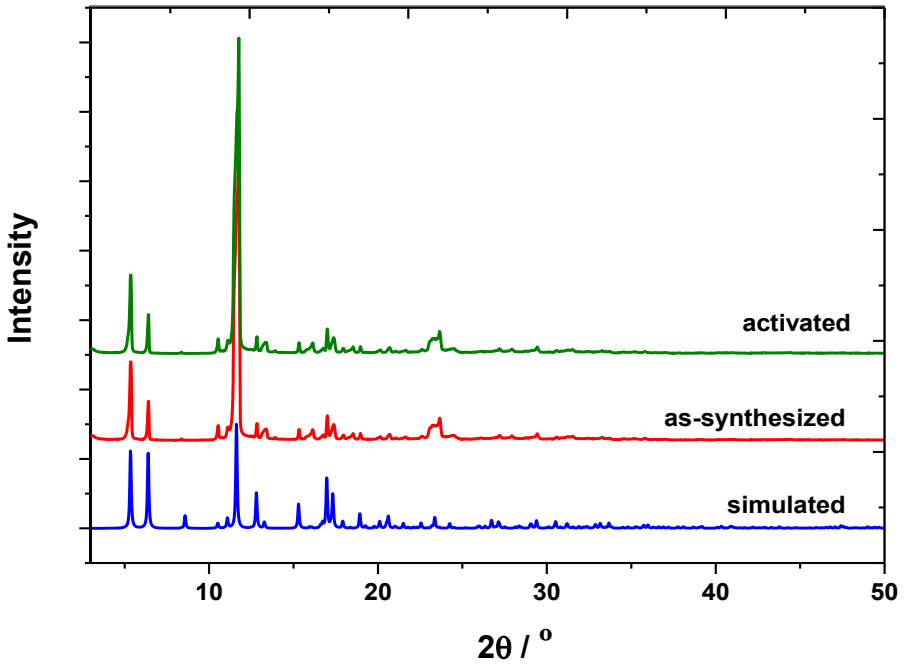

Figure S11. Comparison of the simulated (blue) PXRD pattern with the experimental as-synthesized (red) and activated [guest-free, (green)] PXRD patterns of ZIF-301.

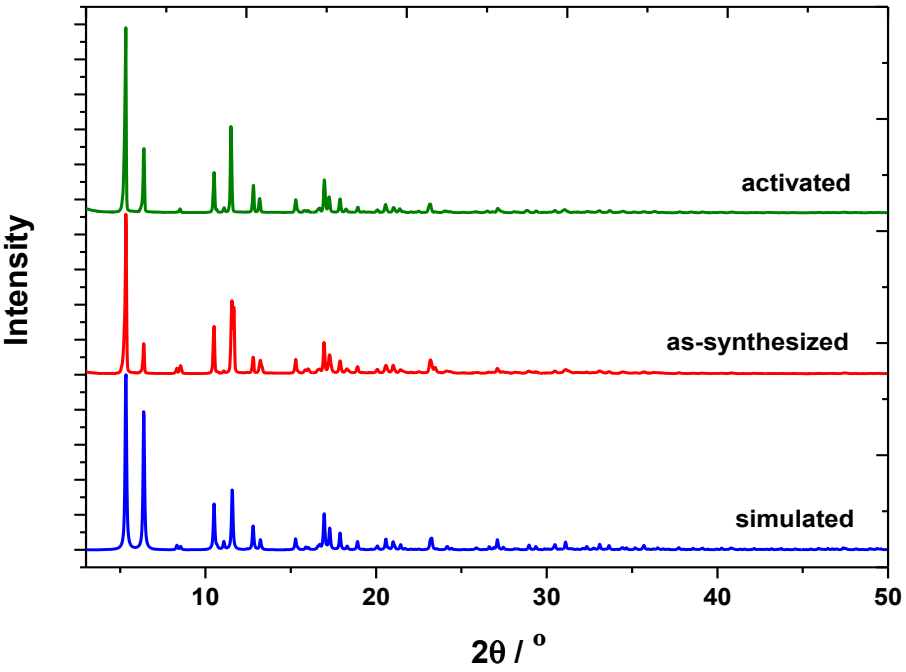

Figure S12. Comparison of the simulated (blue) PXRD pattern with the experimental as-synthesized (red) and activated [guest-free, (green)] PXRD patterns of ZIF-302.

Section S6: Thermal Gravimetric Analyses

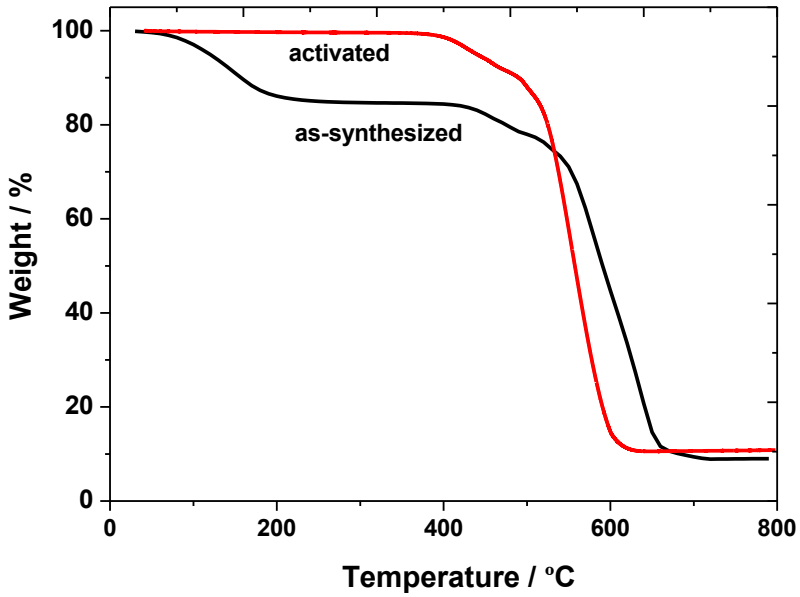

Figure S13. TGA trace for ZIF-300 at a heating rate of 5 °C min^{-1} under air flow.

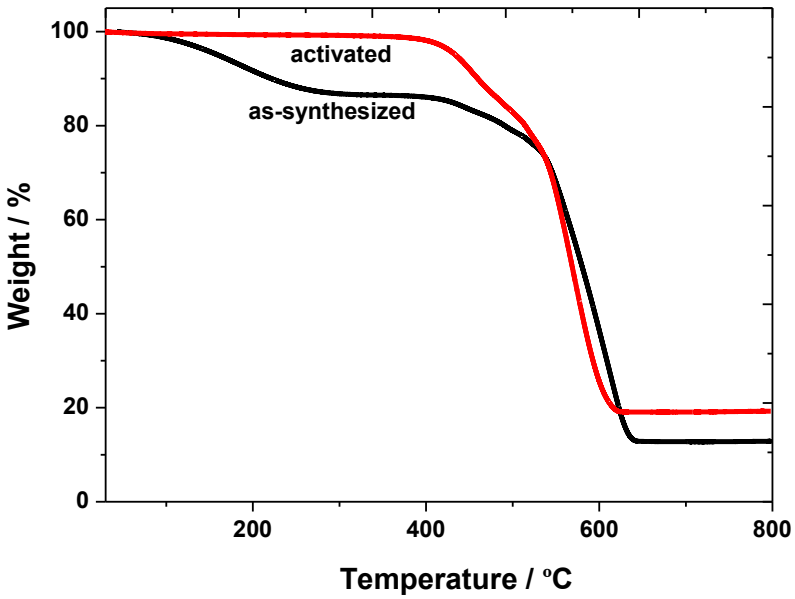

Figure S14. TGA trace for ZIF-301 at a heating rate of 5 °C min^{-1} under air flow.

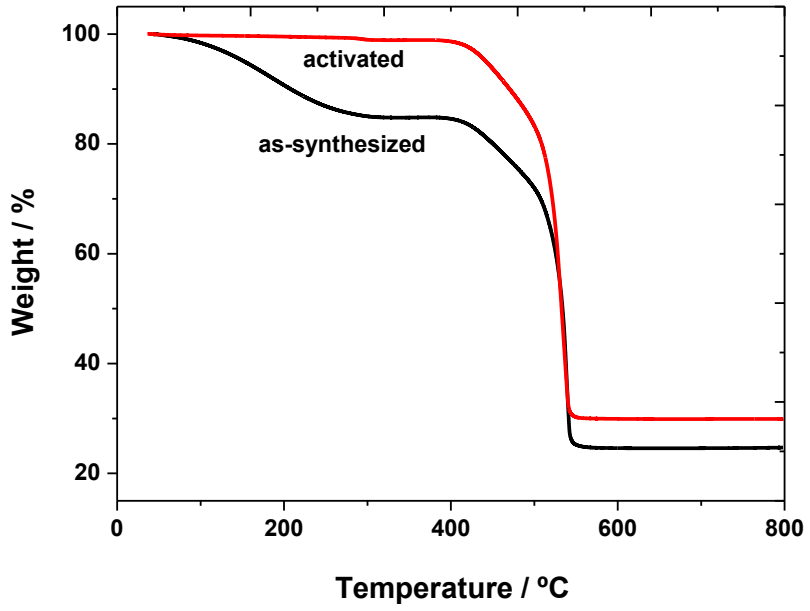

Figure S15. TGA trace for ZIF-302 at a heating rate of 5 °C min^{-1} under air flow.

Section S7: Ar Adsorption Measurements

The permanent porosity of activated ZIFs was proven by Ar sorption analysis. Type-I isotherms were observed for all three ZIFs. The Langmuir (Brunauer-Emmet-Teller) surface areas were 490 (420), 825 (680), and 270 (240) $m^2\ g^{-1}$ for ZIF-300, ZIF-301, and ZIF-302, respectively. It is important to note that these **CHA**-type ZIFs have many disordered imidazolate links, which protrude into the middle of the pore in an interspersed fashion. Accordingly, guest molecules may not be able to effectively pack within the pores to reduce all of the empty space (i.e. loose packing of Ar molecules within the pore). We believe this to be the main culprit for the deviation in the observed surface areas. Indeed, ZIF-302, which has the highest concentration of bIm links among the three ZIFs, shows the lowest porosity.

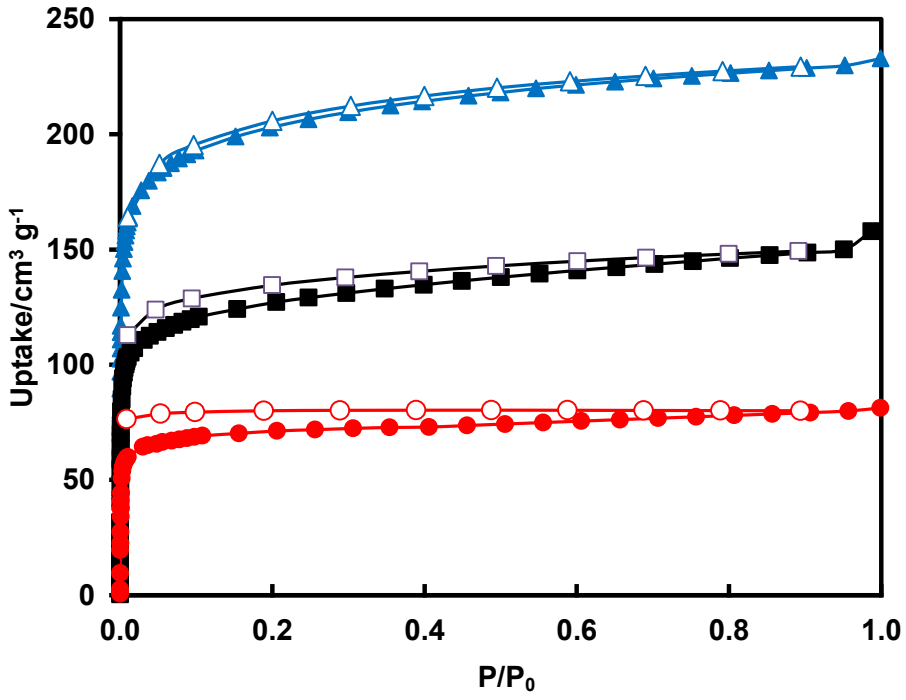

Figure S16. Ar isotherms of ZIF-300 (square), ZIF-301 (triangle), and ZIF-302 (circle) at 87 K. Filled and open symbols represent adsorption and desorption branches, respectively. The connecting curves are guides for the eye.

Section S8: Water Stability and Water Adsorption Measurements

Water stability test:

ZIF-300, -301, and -302 were analyzed for their stability in water at 100 °C over the course of 7 days. The samples' structural stability were routinely checked every 24 h by PXRD analysis. The corresponding PXRD patterns at these designated times for all samples showed that the structure of ZIF-300, -301, and -302 was fully maintained.

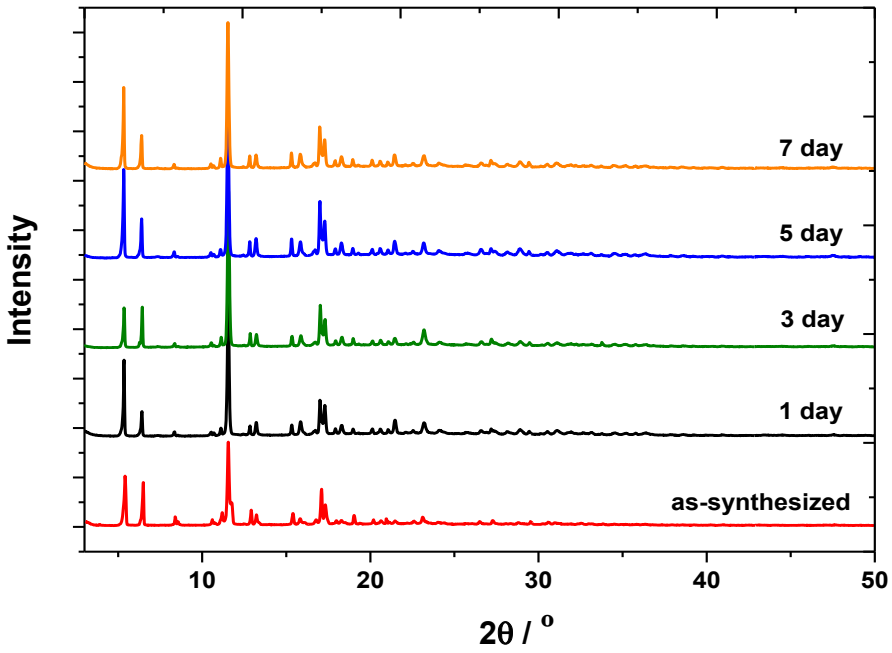

Figure S17. PXRD patterns of ZIF-300 collected after suspension in water at 100 °C over the course of 7 days. The PXRD pattern of as-synthesized ZIF-300 (red) is provided for reference.

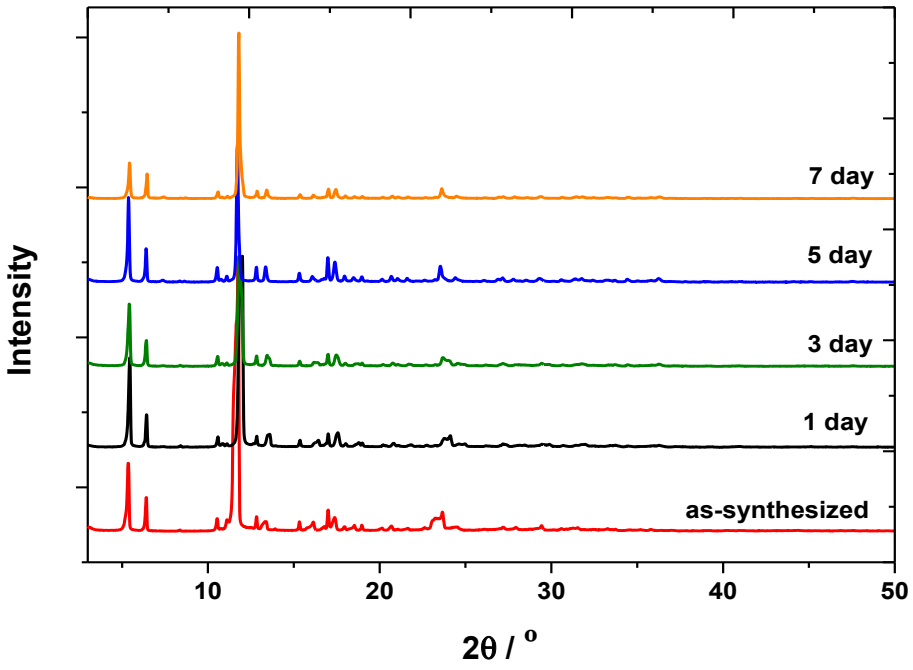

Figure S18. PXRD patterns of ZIF-301 collected after suspension in water at 100 °C over the course of 7 days. The PXRD pattern of as-synthesized ZIF-301 (red) is provided for reference.

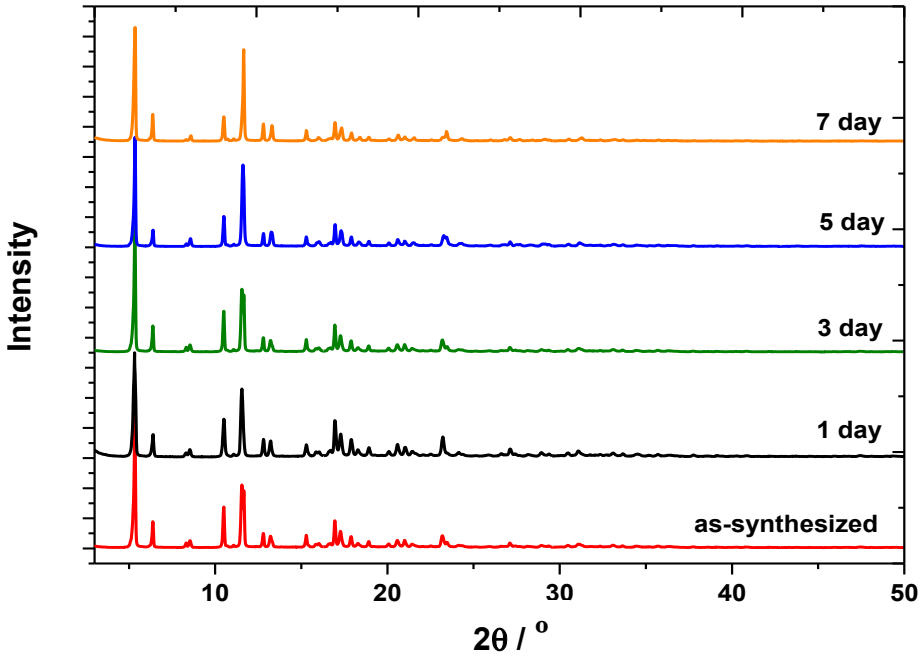

Figure S19. PXRD patterns of ZIF-302 collected after suspension in water at 100 °C over the course of 7 days. The PXRD pattern of as-synthesized ZIF-302 (red) is provided for reference.

Water adsorption isotherm at RT:

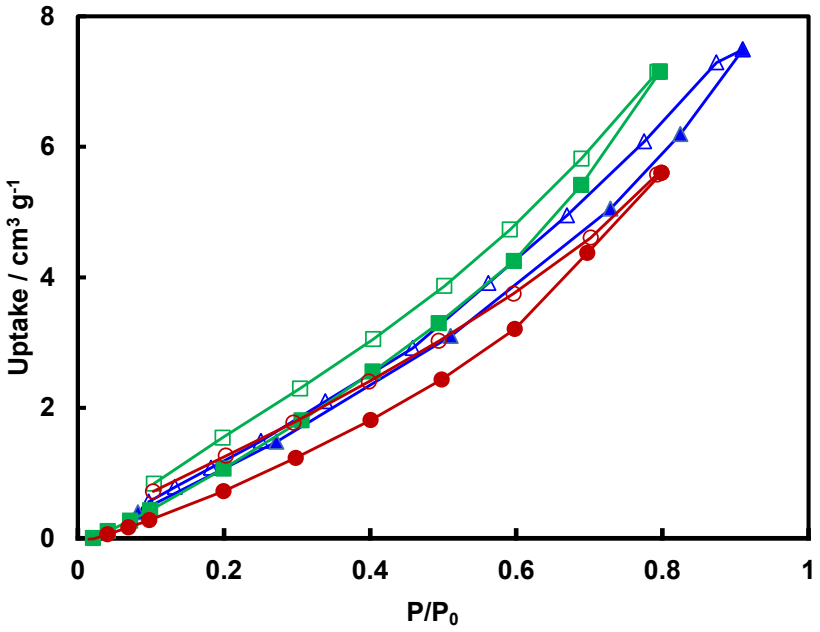

Figure S20. Water isotherm of ZIF-300 (triangle), -301 (square), and -302 (circle) at 298 K. Filled and open symbols represent adsorption and desorption branches, respectively. The connecting curves are guides for the eye.

Section S9: CO_2 Selectivity and Capacity Studies of ZIFs

Gas selectivity calculated by Henry's Law [S1]

Virial-type equation was employed for estimation of Henry's constant:

$$ln\,P = ln\,N + \frac{1}{T}\sum_{i=0}^{m} a_i N^i + \sum_{i=0}^{n} b_i N^i \qquad (1)$$

Where P is pressure, N is the adsorbed amount, T is temperature, a_i and b_i are virial coefficients, and m and n are the number of virial coefficients required for adequate fitting of the isotherms. As a result, Henry's constant (K_H) at the temperature T can be calculated:

$$K_H = \exp(-b_o) \cdot \exp\left(-\frac{a_o}{T}\right) \qquad (2)$$

Based on the estimated K_H, the selectivity of gas component i, from the mixture of two gas components i and j, is calculated as follows:

$$S_{ij} = K_{Hi}/K_{Hj} \qquad (3)$$

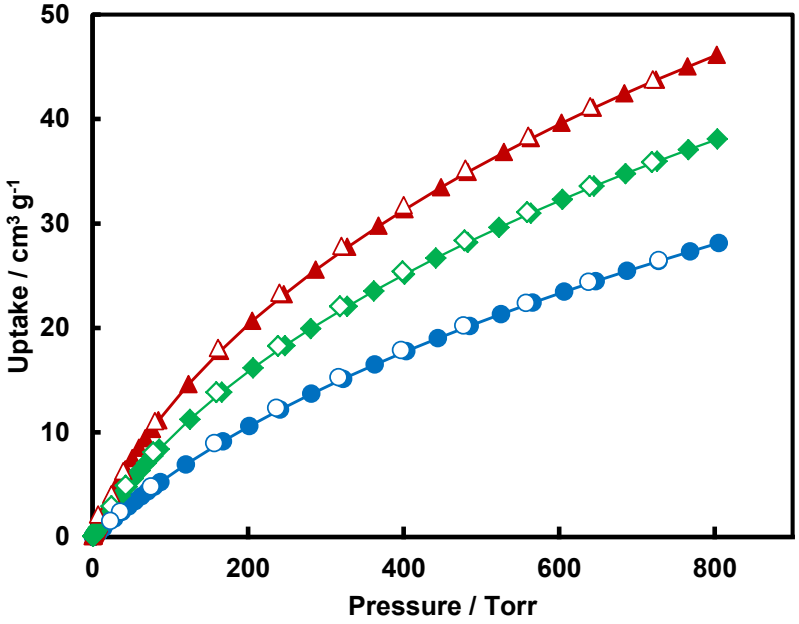

Figure S21. CO_2 isotherms for ZIF-300 at 273 (triangle), 283 (square), and 298 K (circle). Filled and open symbols represent adsorption and desorption branches, respectively. The connecting curves are guides for the eye.

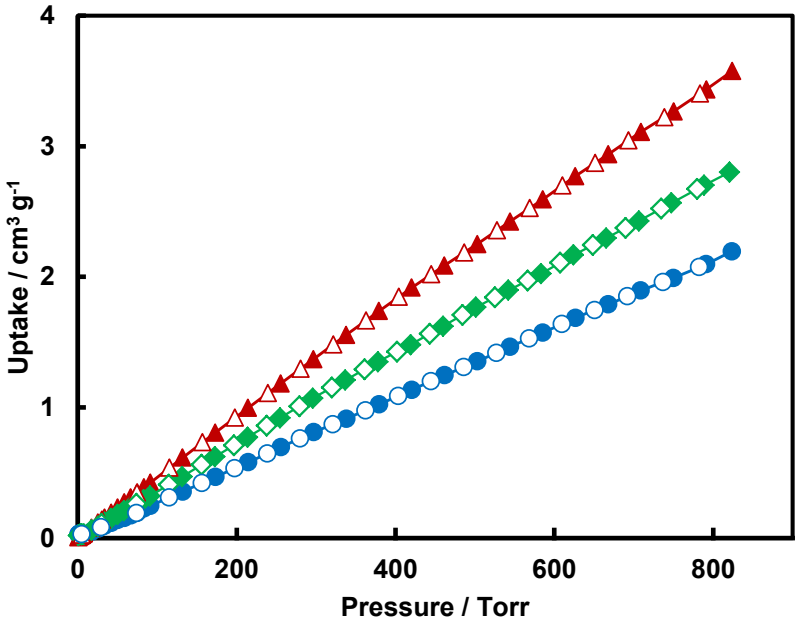

Figure S22. N_2 isotherms for ZIF-300 at 273 (triangle), 283 (square), and 298 K (circle). Filled and open symbols represent adsorption and desorption branches, respectively. The connecting curves are guides for the eye.

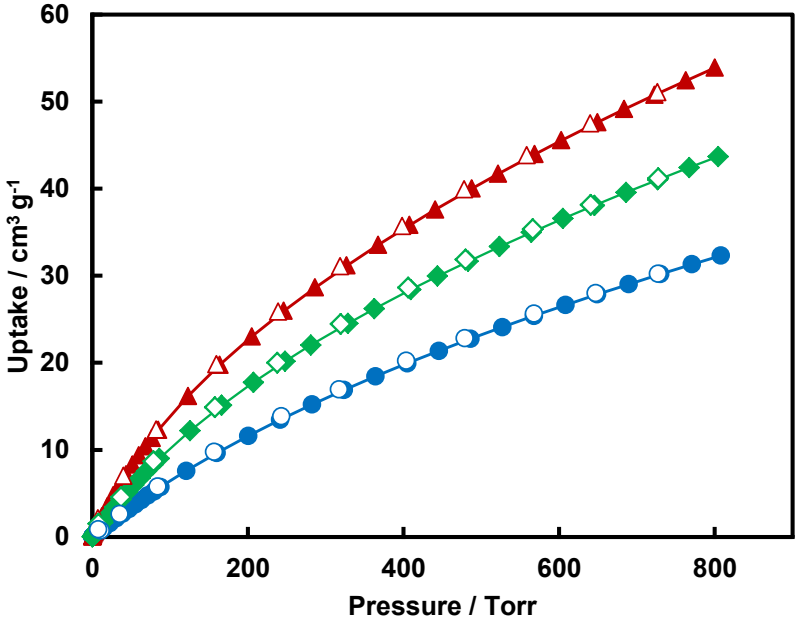

Figure S23. CO_2 isotherms for ZIF-301 at 273 (triangle), 283 (square), and 298 K (circle). Filled and open symbols represent adsorption and desorption branches, respectively. The connecting curves are guides for the eye.

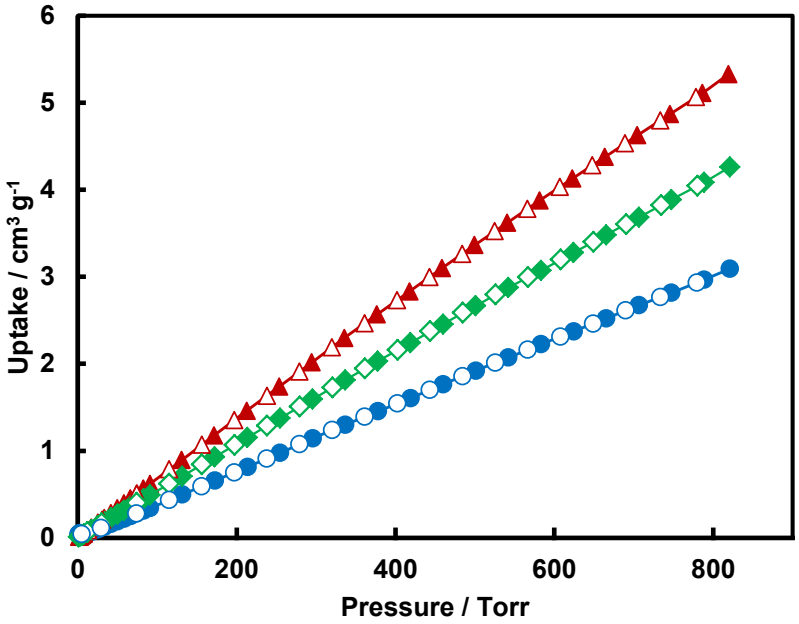

Figure S24. N_2 isotherms for ZIF-301 at 273 (triangle), 283 (square), and 298 K (circle). Filled and open symbols represent adsorption and desorption branches, respectively. The connecting curves are guides for the eye.

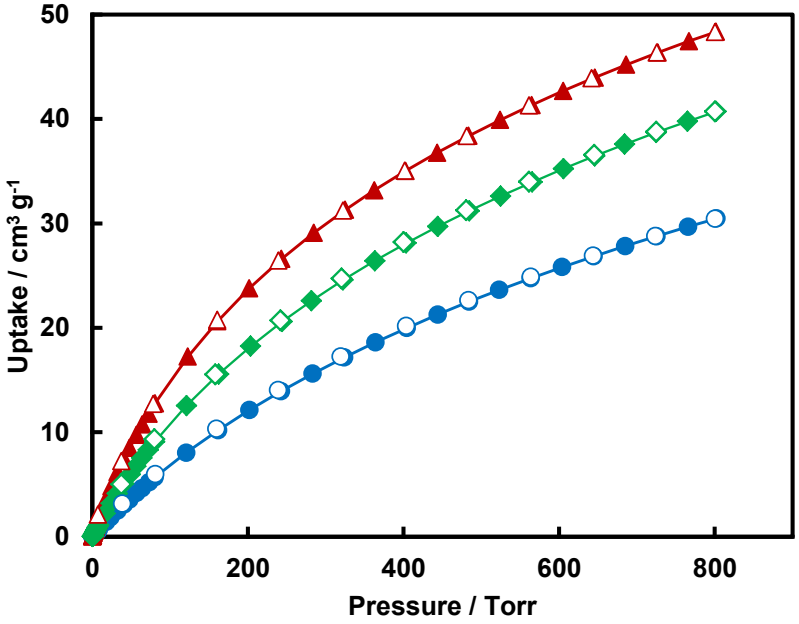

Figure S25. CO_2 isotherms for ZIF-302 at 273 (triangle), 283 (square), and 298 K (circle). Filled and open symbols represent adsorption and desorption branches, respectively. The connecting curves are guides for the eye.

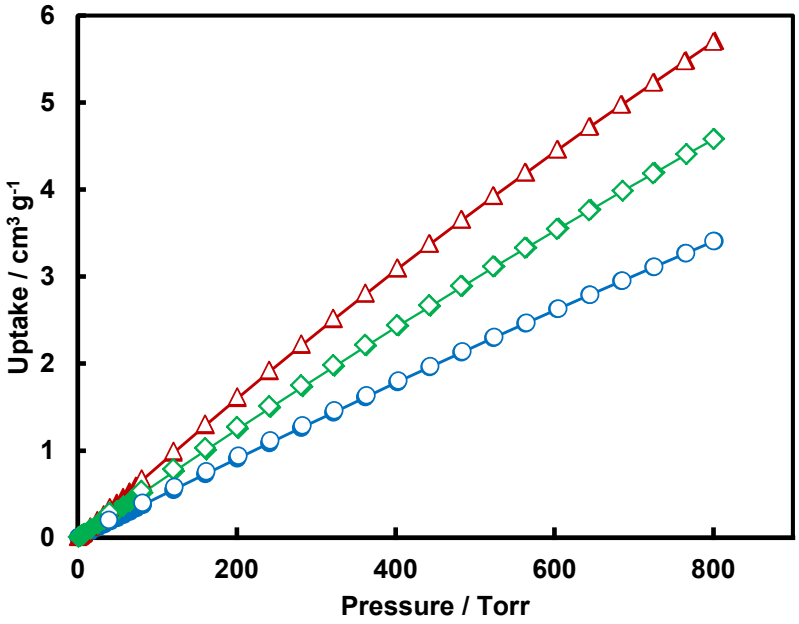

Figure S26. N_2 isotherms for ZIF-302 at 273 (triangle), 283 (square), and 298 K (circle). Filled and open symbols represent adsorption and desorption branches, respectively. The connecting curves are guides for the eye.

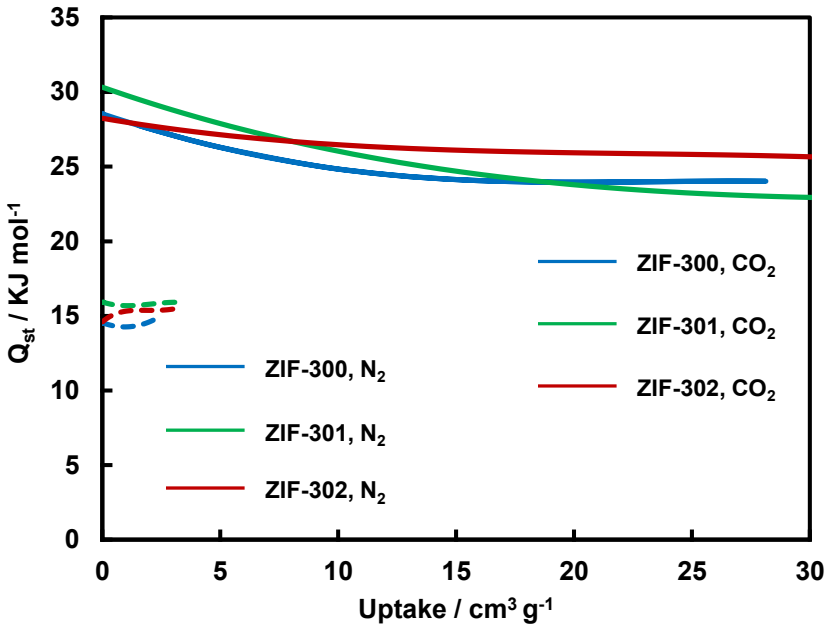

Figure S27. The isosteric heat of adsorption of CO_2 (solid lines) and N_2 (dashed lines) for ZIF-300 (blue), -301 (green), and -302 (red).

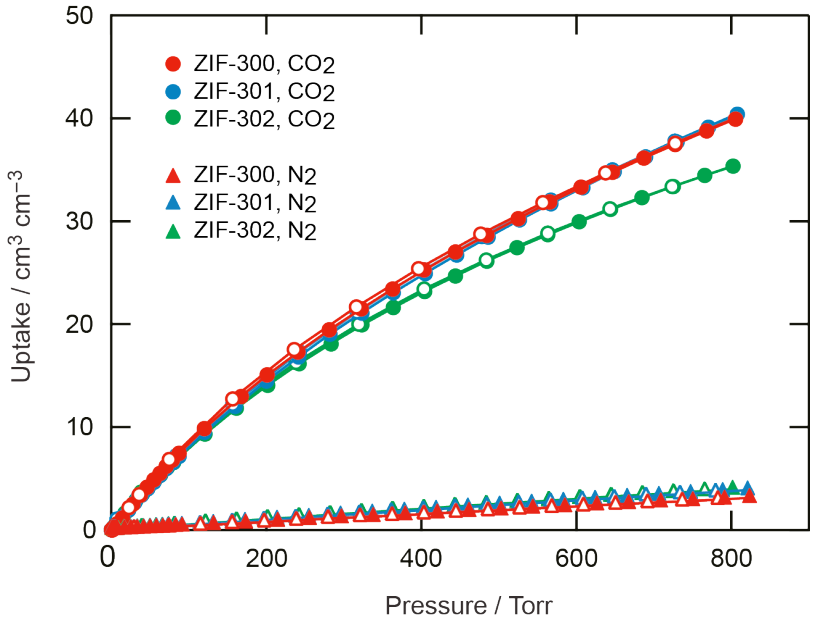

Figure S28. CO_2 (circles) and N_2 (triangles) isotherms of ZIF-300 (red), -301 (blue), and -302 (green) at 298 K. Filled and open symbols represent adsorption and desorption branches, respectively.

Section S10: Breakthrough Measurements

Breakthrough experiments on **CHA**-type ZIFs were performed according to a published procedure.[S2] The experiments under dry conditions were carried out by flowing a mixture of CO_2/N_2 at 8.4 : 1.6 sccm through a bed containing activated ZIF materials (1.06, 0.788, and 1.20 g for ZIF-300, -301, and -302, respectively). Effluent from the bed was monitored by mass spectrometry, and breakthrough time was recorded as 5% of the feed concentration of CO_2 was trapped in the bed. For wet breakthrough experiments, the sample was purged first by a wet N_2 stream (80% RH) until water saturation was detected. Then, dry CO_2 flow was introduced and breakthrough experiments were implemented. Breakthrough time was corrected by subtracting the time to breakthrough for a blank column.

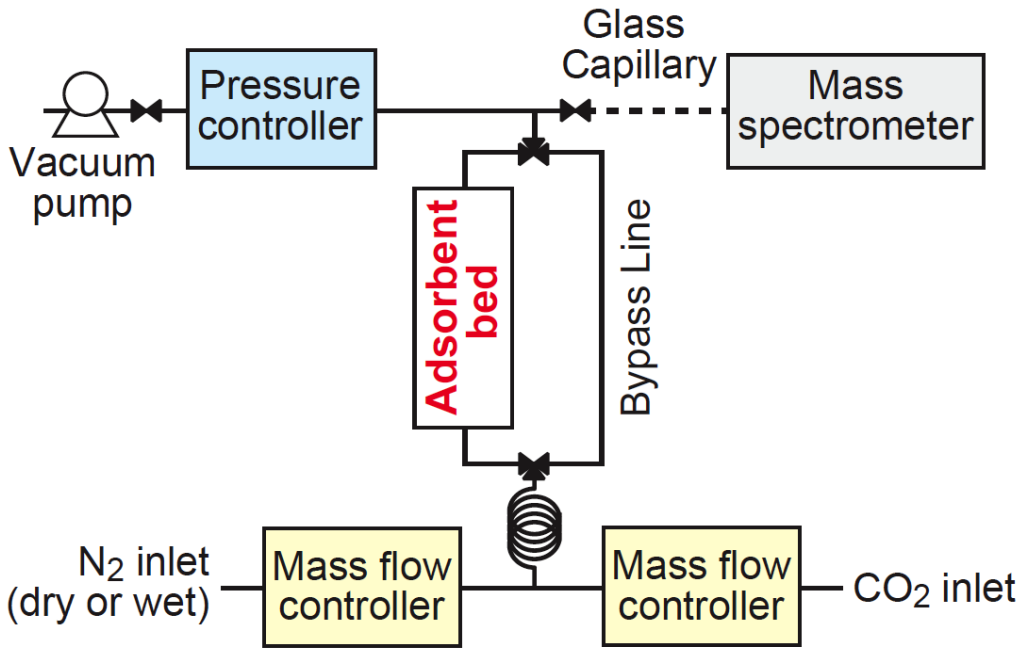

Figure S29. Schematic representation of breakthrough experimental setup.

Table S4. Average breakthrough time (n = 3) and CO_2 uptake capacity under dry and wet conditions of ZIF-300, -301, and -302

Materials	Average breakthrough time (n =3)		CO_2 uptake capacity	
	Dry (sec)	Wet (sec)	Dry (cm^3 cm^{-3})	Wet (cm^3 cm^{-3})
ZIF-300	269	264	10.4	10.2
ZIF-301	237	244	8.0	8.2
ZIF-302	174	175	5.5	5.6

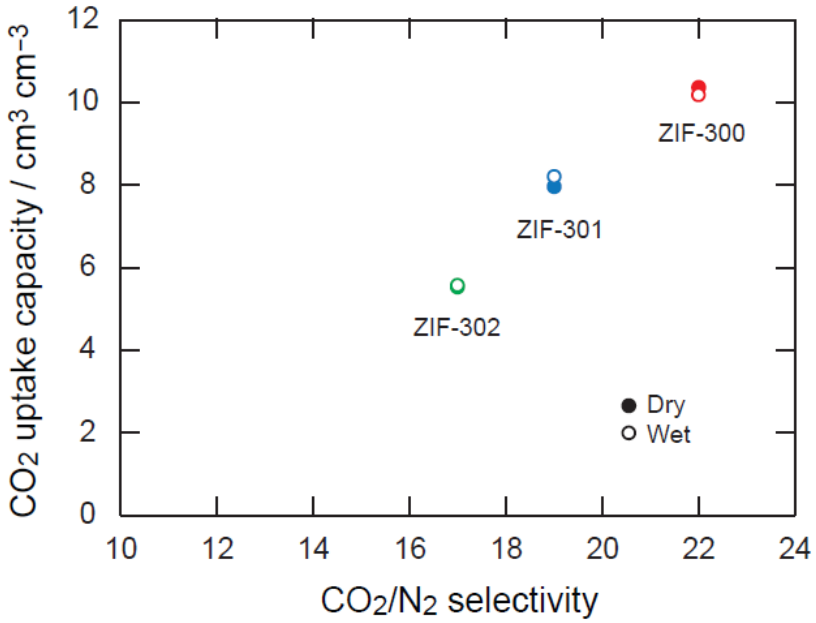

Figure S30. Relationship between CO_2/N_2 selectivity and dynamic CO_2 uptake capacity for **CHA**-type ZIFs.

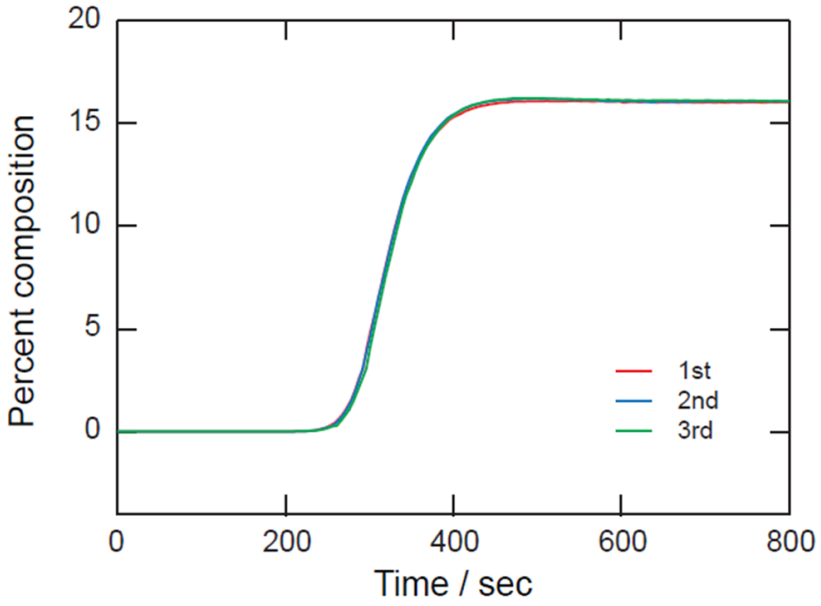

Figure S31. CO_2 breakthrough curves of ZIF-300 under dry conditions.

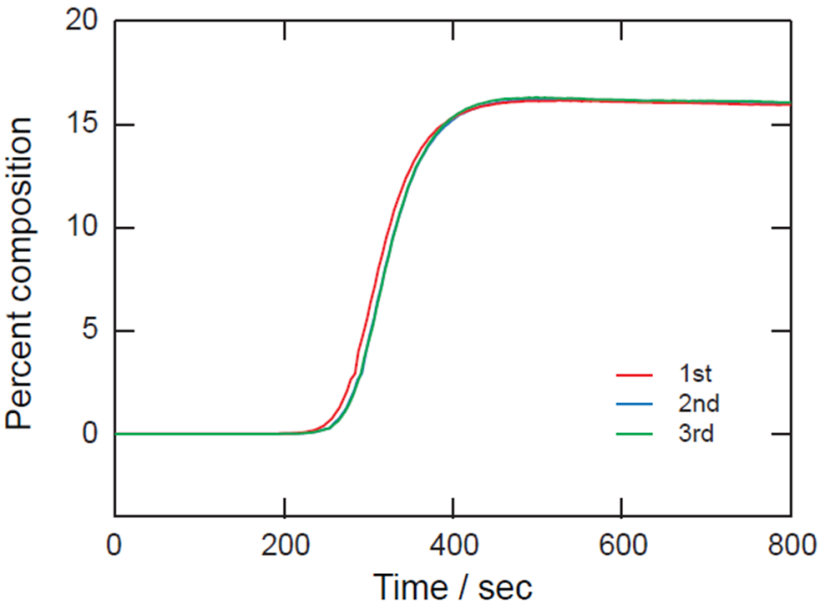

Figure S32. CO_2 breakthrough curves of ZIF-300 under wet conditions.

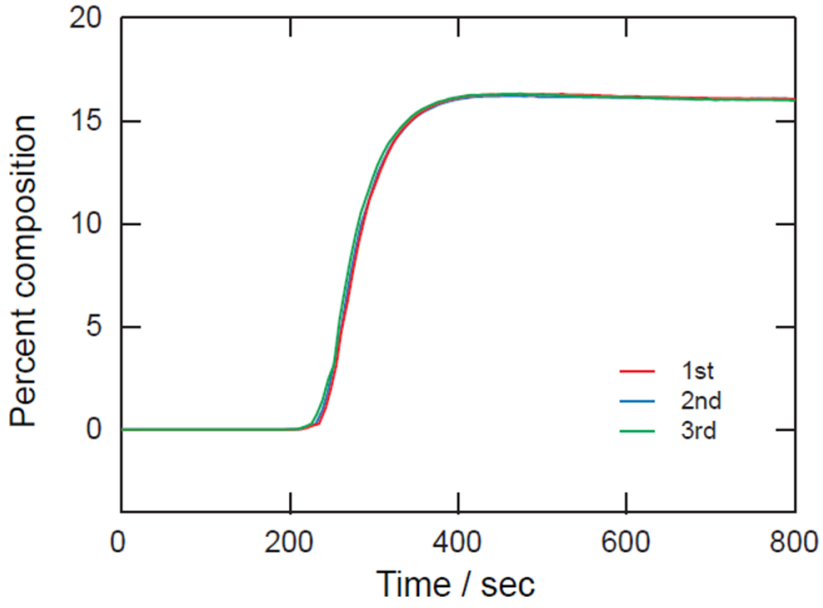

Figure S33. CO_2 breakthrough curves of ZIF-301 under dry conditions.

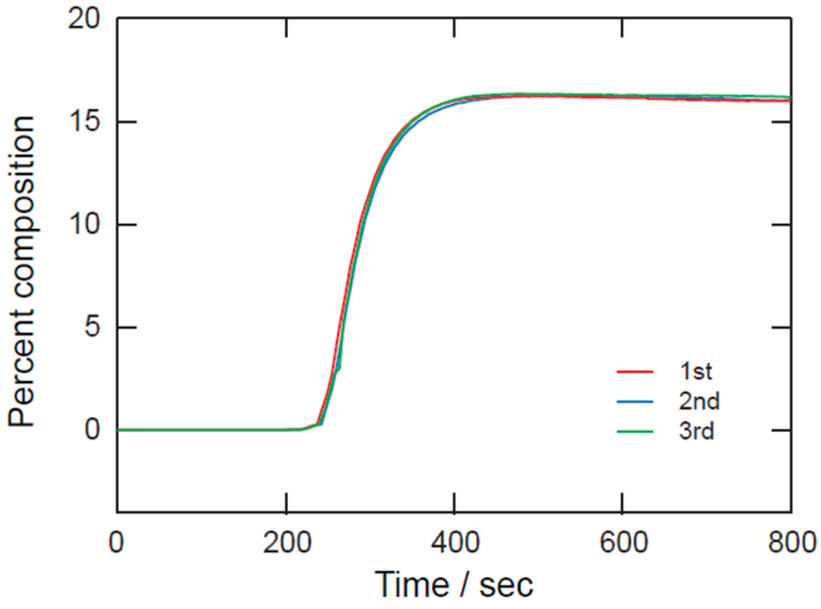

Figure S34. CO_2 breakthrough curves of ZIF-301 under wet conditions.

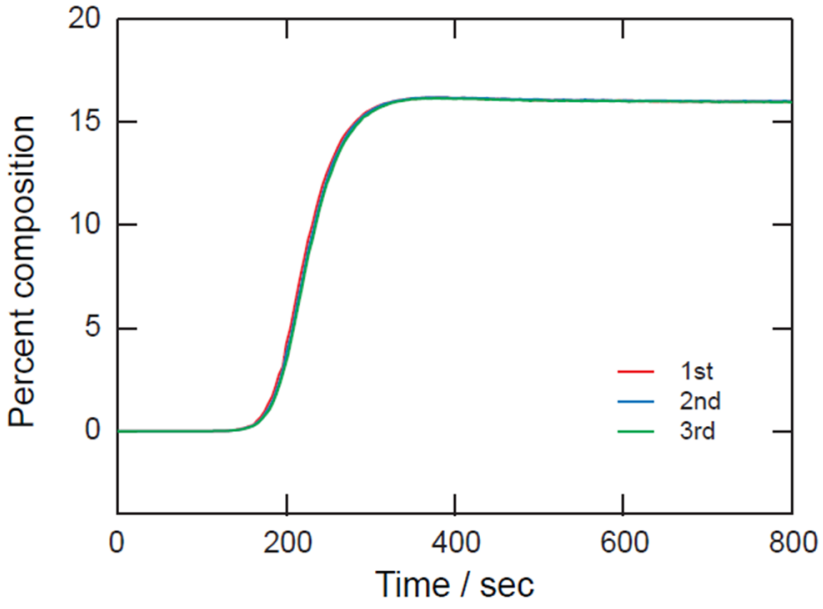

Figure S35. CO_2 breakthrough curves of ZIF-302 under dry conditions.

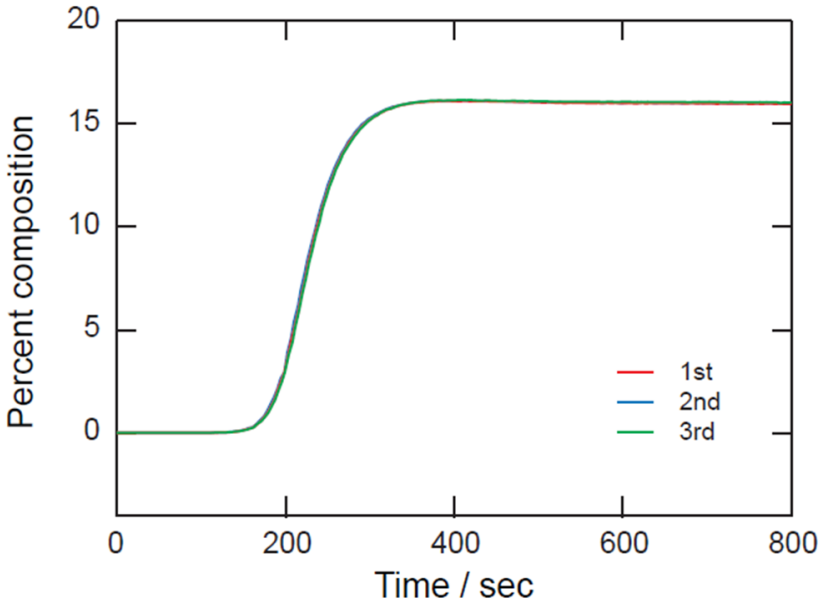

Figure S36. CO_2 breakthrough curves of ZIF-302 under wet conditions.

Section S11: References

[S1] L. Czepirski, J. JagieŁŁo, *Chem. Eng. Sci.* **1989**, *44*, 797–801.

[S2] D. Li, H. Furukawa, H. Deng, C. Liu, O. M. Yaghi, D. S. Eisenberg, *Proc. Natl. Acad. Sci. U.S.A.* **2014**, *111*, 191–196.